



Open Archive TOULOUSE Archive Ouverte (OATAO)

OATAO is an open access repository that collects the work of Toulouse researchers and makes it freely available over the web where possible.

This is an author-deposited version published in : <http://oatao.univ-toulouse.fr/>
Eprints ID : 13830

To cite this version : Fabacher, Emilien and Lizy-Destrez, Stéphanie and Alazard, Daniel and Ankersen, Finn [Guidance and navigation for electromagnetic formation flight orbit modification](#).
In: EuroGNC, 13 April 2015 - 15 April 2015 (Toulouse, France)

Any correspondence concerning this service should be sent to the repository administrator: staff-oatao@listes-diff.inp-toulouse.fr

Guidance and Navigation for Electromagnetic Formation Flight Orbit Modification

Emilien Fabacher, Stéphanie Lizy-Destrez, Daniel Alazard, Finn Ankersen and Jean-François Jourdas

Abstract Electromagnetic formation flight (EMFF) is a recent concept, aiming to control relative motions of formation flying satellites using magnetic interactions. Each satellite is equipped with a magnetic dipole. The formation degree of cooperation, depending on the ability of each spacecraft to control its dipole and its attitude, has a great impact on the methods used to perform the formation GNC. This paper describes results obtained in the case of semi-cooperative EMFF composed of a chaser and a target, in the field of navigation and guidance. Preliminary studies indicate that the target relative position and attitude can be determined while measuring the magnetic field at the chaser location, and the acceleration of this chaser. Focus is also made on the guidance for the whole formation orbit transfer, if only the chaser has thrust capacity: theory shows that geometrical configurations exist for which the formation is in an equilibrium state.

1 Formation flight and electromagnetic actuation

Electromagnetic actuators have been used in space for 50 years [15]. This technology is still often employed to control the attitude of a spacecraft, using magnetorquers (or torque rods). Those devices enable the spacecraft to create a magnetic field which interacts with the Earth magnetic field. Thanks to this interaction, a torque is applied to the satellite. Because of their reliability and simplicity, they are particularly used in safe mode. Magnetorquers also enable to unload momentum accumulated in reaction wheels [5].

Emilien Fabacher, Stéphanie Lizy-Destrez, Daniel Alazard
SUPAERO, 10 av. Edouard Belin, 31000 Toulouse, FRANCE, e-mail: emilien.fabacher@isae.fr

Finn Ankersen
ESTEC, Keplerlaan 1, 2201 AZ Noordwijk, THE NETHERLANDS

Jean-François Jourdas
Airbus DS, 66 route de Verneuil, 78130 Les Mureaux, FRANCE

Satellites formation flying is not a recent concept. Several formation flying missions have already been successful: CLUSTER mission for example is based on four satellites flying in a tetrahedral formation to study the Earth magnetic field. However it is only recently, with PRISMA mission for example, that satellites have demonstrated the ability to fly in very close formation (a few tens of meters) [7]. This new possibility is highly attractive for many new concepts. For instance, the opportunities offered by the flexible architecture of fractionated spacecraft are continuously increasing [3]. At the same time, distance based applications like interferometry represent a very interesting field, which would greatly benefits from very close formation flying.

Many disturbances exist in low Earth orbit: atmospheric drag, solar pressure, differential accelerations due to the J_2 coefficient of the Earth gravity model. . . These disturbances cause even a perfectly positioned formation to drift apart if nothing is done. Therefore, formation flying implies to find a way to stay in formation, i.e. to apply accelerations to each one of the formation spacecrafts. Up to now, the only way translational accelerations are created in space is by thrusters. However, thrusters require propellant, which in turn means that the formation has a finite lifetime due to the limited amount of propellant carried aboard each spacecraft. For this reason amongst others, flying in formation using magnetic interactions would be a great advantage.

This paper develops a framework for guidance and navigation applied to electromagnetic formation flying (EMFF). Section 2 first defines the different types of EMFF scenarios existing. Section 3 describes the state of the art concerning EMFF. A detailed justification of the work realised in this study is developed in section 4. The following then clearly details the techniques developed: section 5 defines the magnetic models used to describe magnetic interactions. Section 6 then presents a way to determine the relative position and attitude of the target using only magnetometers and accelerometers. Finally, section 7 deals with determining the possible formation configurations to assure its equilibrium during the orbital transfer.

2 Electromagnetic formation flight scenarios

Different electromagnetic formation flight scenarios exist. The simplest one is formation flying satellites which have been designed to work together: each one is equipped with electromagnetic actuators and they are used together to create the forces needed to maintain the formation. This scenario will be called “Fully-cooperative electromagnetic formation flight”. It will be described more in detail in part 3.1.

Part 3.2 will present the “Semi-cooperative electromagnetic formation flight” scenario. This one is based on the interaction between one satellite called “chaser”, and another called “target”. While the chaser is designed to realise EMFF, the target is not. The target is only supposed to be equipped with a magnetic dipole, which is constant in time in the target body frame.

A “Non-cooperative electromagnetic formation flight” scenario would describe the interaction between a chaser satellite equipped with electromagnetic actuators and a target considered not to be equipped with any. This scenario is not developed in this paper, because the science it relies on considerably differs from the one the two others are based upon. Indeed, while the fully- and semi-cooperative scenarios can correctly be described by magneto-statics, the non-cooperative one relies essentially on induction and eddy currents.

3 EMFF literature

The following section develops the works already realised on EMFF.

3.1 *Fully-cooperative EMFF*

Many concepts have been proposed regarding fully cooperative EMFF. The Space Systems Laboratory of Massachusetts Institute of Technology (MIT SSL) is working on formations composed of N identical spacecrafts, equipped with steerable dipoles [10]. JAXA published on fractionated spacecrafts composed of one central body and several smaller deployable systems [16]. Thales Alenia Space considered controlling the position of small modules carrying steerable dipoles around a central body equipped with a rotating permanent dipole [6].

Kong proposed in 2004 to use EMFF to control the relative position of spacecraft composing NASA's Terrestrial Planets Finder telescope [8].

Kwon analysed in 2005 the performance of a satellite array composed of two to N satellites. The main objective was to demonstrate the capacity to remain in a rotating formation, used for example for space telescopes [9].

To compensate the accumulating torque due to the interaction between constant magnetic dipoles and the Earth magnetic field, Sakai proposed to wave the dipoles strength, and control the phase between the two dipoles in order to modulate the force [13].

Much work has already been realised on EMFF guidance and control, particularly on formation in which every satellite is equipped with the same steerable dipole.

Schweighart solved in 2008 the dipole planning problem for an N -spacecraft formation flight. His work enables to obtain the dipole one should apply to each spacecraft flying in the formation, in order to realise a given trajectory [14].

Ahsum worked on the stability of the N -spacecraft formation, and proposed ways to find time-optimal trajectories in 2007 [1].

Buck worked on under-actuated formations in 2013. His focus was on the stability of the system composed of two satellites only, considering that they do not carry steerable dipoles, but only one axis modular dipole, and torque capacity [4].

3.2 *Semi-cooperative EMFF*

Until now, only fully cooperative control has really been studied, meaning that both the target and the chaser are actuated. The possibility to externally control the attitude and orbit of a satellite using electromagnetic actuators seems therefore a novel idea, which is interesting for several reasons:

- The question of satellite servicing has been progressively raised since 2000 [12].
- Many satellite missions come to an end due to the lack of fuel, but could work much longer if their attitude and orbit were controlled.

Many satellites are equipped with magnetorquer to control their attitude, which makes EMFF an easy option. Indeed, these magnetic device could be used by an EMFF chaser to control the attitude and orbit of the target. The presence of a magnetic dipole on a target would provide the chaser a possibility to exert forces and torques on this target. Magnetic actuators could therefore be used to control the attitude of a target, as well as its orbit, without the need of any contact between the two satellites. EMFF would moreover offer a possibility for satellites having lost de-orbit capacity to nonetheless respect the different laws and recommendations on the matter.

This context made Voirin propose in 2012 to use electromagnetic interaction to attract a satellite in which a remaining magnetic dipole would be present [18].

4 Formation orbit modification

Let's consider fully-cooperative EMFF. As said in section 1, many disturbances exist in Earth orbit, specially at low altitude. These disturbances do not only modify the geometry of a formation. Indeed, they also have an impact on the formation Center of Mass (CoM). For example, atmospheric drag decreases the altitude of the orbit, J_2 coefficient of the gravity has an impact on the orbital plane. . . Because of these perturbations, maintaining the orbit of the formation would be necessary for a long mission.

Controlling the absolute orbit of the formation is even more important for semi-cooperative EMFF. Indeed, as presented in section 3.2, modify the absolute orbit of a target while controlling its attitude is the core of the semi-cooperative EMFF concept.

To sum up, an EMFF mission would need a way to control its orbit whatever the scenario. This in turn means that at least one member of the formation needs to have thrust capacity. If every member is equally equipped with thrusters, then the magnetic control could be turned off during the orbit modification. It could be the case for fully-cooperative formation flight. If on the contrary only some of the satellites composing the formation are equipped with thrusters, then magnetic control would be very important during orbit modification, in order to modify the orbit of the complete formation and not only of the spacecraft equipped with thrusters. This would

be the case for semi-cooperative formation flight, but could also be applicable to fully-cooperative EMFF, depending on the architecture chosen.

This study focuses on a semi-cooperative formation composed of two satellites. While the chaser is equipped with an attitude and orbit control system (AOCS), the target is not. It is therefore unable to control its attitude and its orbit. The only assumption is that it is equipped with a fixed magnetic dipole, created for example by magnetorquers. In this case, modifying the orbit of the formation is not a simple task. When decomposing it into steps, one can identify the followings, which all represent challenges:

- **Navigation:** the chaser needs to know the relative position and attitude of the target. In the case of fully cooperative EMFF, it may not represent a great challenge, thanks to possible communications between the two satellites. In the case of semi-cooperative EMFF on the other hand, it would represent a critical challenge.
- **Detumbling:** in the case of semi-cooperative EMFF, the target may be tumbling at the beginning of the interaction. In this case, detumbling it before trying to modify the orbit of the formation appears to be a good idea.
- **Reconfiguration:** In order to realise the orbit modification, some geometrical configurations may be more interesting than others. In this case, the chaser would have to modify the relative attitude and position of the target, while staying in formation.
- **Orbit modification:** The issue raised by the orbit modification is to ensure the stability of the formation.

These steps are not necessarily successive. The navigation, for example, would work continuously during the whole mission. However, in a de/re-orbit mission, as it has been proposed by Voirin [18], they would start successively in the order presented in figure 1: the chaser would approach the target, without having any influence on it. It would then first precisely assess the relative position and attitude of its target, before detumbling it, reconfiguring the geometry and then pushing or pulling it. The following presents preliminary results concerning the navigation and



Fig. 1 Steps realised by the chaser during a de/re-orbit mission.

the guidance during orbit transfer. Indeed, the techniques developed for these two tasks are very similar, as it will be seen.

5 Magnetic model

Let's consider two coils used to create a magnetic field. The following develops a first approximation of the force created by one coil on the other.

The magnetic field created by a coil through which a current i_1 is passing is given by the Biot - Savart law:

$$\mathbf{B}_1(\mathbf{s}) = \frac{\mu_0 N_1 i_1}{4\pi} \oint \frac{\mathbf{dl} \times \hat{\mathbf{r}}}{\|\mathbf{r}\|^2} \quad (1)$$

With:

μ_0	the magnetic permeability of the void ($\mu_0 = 4\pi \cdot 10^{-7} \text{ kg.m}/(\text{A}^2.\text{s}^2)$),
N_1	the number of turn in coil 1,
i_1	the current in coil 1 (A),
\mathbf{dl}	the elementary vector on the coil,
\mathbf{r}	the vector from a point on the coil to the point considered,
$\hat{\mathbf{r}}$	the elementary vector from a point on the coil to the point considered,
\mathbf{s}	the vector from coil center to the point considered.

5.1 Expression of force and torque between two dipoles

The force on an element of conductor \mathbf{dl}_2 through which passes a current i_2 and surrounded by a magnetic field \mathbf{B}_1 is:

$$\mathbf{dF} = i_2 \mathbf{dl}_2 \times \mathbf{B}_1 \quad (2)$$

Integrating (2) on the coil yields:

$$\mathbf{F}_{1/2} = N_2 i_2 \oint \mathbf{dl}_2 \times \mathbf{B}_1 \quad (3)$$

We can then derive the complete expression of the force created by coil 1 on coil 2:

$$\mathbf{F}_{1/2}(\mathbf{s}) = \frac{\mu_0 N_1 i_1 N_2 i_2}{4\pi} \oint \left(\oint \frac{\hat{\mathbf{r}} \times \mathbf{dl}_1}{\|\mathbf{r}\|^2} \right) \times \mathbf{dl}_2 \quad (4)$$

The torque created by coil 1 on coil 2 is derived similarly:

$$\boldsymbol{\tau}_{1/2}(\mathbf{s}) = \frac{\mu_0 N_1 i_1 N_2 i_2}{4\pi} \oint \mathbf{a}_2 \times \left(\left(\oint \frac{\hat{\mathbf{r}} \times \mathbf{dl}_1}{\|\mathbf{r}\|^2} \right) \times \mathbf{dl}_2 \right) \quad (5)$$

Because these expressions are not very easy to use, several other expressions have been derived [14], [17]. They describe the force and torque created by a magnetic

dipole on another one. The exact expressions, called “close field” expressions because valid even very close to the magnetic devices are given by equation (4) and (5). The “far field” expressions are first-term Taylor expansion of the close field expressions. They are reliable when the distance between the dipoles is larger than 6 to 8 coils radii.

The far field expression of the magnetic field is given by equation (6) [17]:

$$\mathbf{B}_1 = \frac{\mu_0}{4\pi d^3} (3(\boldsymbol{\mu}_1 \cdot \hat{d})\hat{d} - \boldsymbol{\mu}_1) \quad (6)$$

Force and torque between two magnetic dipoles in “far field” are given by equation (7) and (8).

$$\mathbf{F}_{1/2} = \frac{3\mu_0}{4\pi d^4} ((\boldsymbol{\mu}_1 \cdot \boldsymbol{\mu}_2)\hat{d} + (\boldsymbol{\mu}_1 \cdot \hat{d})\boldsymbol{\mu}_2 + (\boldsymbol{\mu}_2 \cdot \hat{d})\boldsymbol{\mu}_1 - 5(\boldsymbol{\mu}_1 \cdot \hat{d})(\boldsymbol{\mu}_2 \cdot \hat{d})\hat{d}) \quad (7)$$

$$\boldsymbol{\tau}_{1/2} = \boldsymbol{\mu}_2 \times \mathbf{B}_1 = \boldsymbol{\mu}_2 \times \left(\frac{\mu_0}{4\pi d^3} (3(\boldsymbol{\mu}_1 \cdot \hat{d})\hat{d} - \boldsymbol{\mu}_1) \right) \quad (8)$$

With:

- $\mathbf{F}_{1/2}$ the force from dipole 1 on dipole 2 (N),
- $\boldsymbol{\tau}_{1/2}$ the torque from dipole 1 on dipole 2 ($N.m$),
- $\boldsymbol{\mu}_1, \boldsymbol{\mu}_2$ the two magnetic dipoles ($A.m^2$),
- d the distance between the two dipoles (m),
- \hat{d} the unitary vector from $\boldsymbol{\mu}_1$ to $\boldsymbol{\mu}_2$.

Note: For expression (7) to be valid, \mathbf{d} must be the vector \mathbf{d}_{12} from dipole 1 to dipole 2. Taking $\mathbf{d} = \mathbf{d}_{21}$ leads to a false expression.

5.2 Matrix expressions

In this section, the force and the torque induced by one magnetic dipole on another will be expressed as matrix products.

5.2.1 Force and torque expressions

Let's write $\frac{\boldsymbol{\mu}_1}{\|\boldsymbol{\mu}_1\|} = [a \ b \ c]^T$ and $\frac{\boldsymbol{\mu}_2}{\|\boldsymbol{\mu}_2\|} = [e \ f \ g]^T$. We also define $\mathbf{d} = d\hat{d} = d[x \ y \ z]^T$, with:

$$x^2 + y^2 + z^2 = 1 \quad (9)$$

Then the force exerted by dipole 1 on dipole 2 can be written:

$$\mathbf{F}_{1/2} = \frac{3\mu_0}{4\pi d^4} \boldsymbol{\mu}_1 \Phi_1 \boldsymbol{\mu}_2 \quad (10)$$

With:

$$\Phi_1(\hat{d}, \hat{\mu}_1) = \begin{bmatrix} 2ax & ay+bx & az+cx \\ ay+bx & 2by & bz+cy \\ az+cx & bz+cy & 2cz \end{bmatrix} - (ax+by+cz) \begin{bmatrix} 5x^2-1 & 5xy & 5xz \\ 5xy & 5y^2-1 & 5yz \\ 5xz & 5yz & 5z^2-1 \end{bmatrix} \quad (11)$$

Similarly, the torque exerted by dipole 1 on dipole 2 is written:

$$\tau_{1/2} = \frac{\mu_0}{4\pi d^3} \mu_2 \times \beta \mu_1 \quad (12)$$

With:

$$\beta(\hat{d}) = \begin{bmatrix} 3x^2-1 & 3xy & 3xz \\ 3xy & 3y^2-1 & 3yz \\ 3xz & 3yz & 3z^2-1 \end{bmatrix} \quad (13)$$

The expression of the magnetic field is simply:

$$\mathbf{B}_1 = \frac{\mu_0}{4\pi d^3} \beta \mu_1 \quad (14)$$

5.2.2 Proof

Starting from equation (8), we can write:

$$\begin{aligned} \frac{4\pi d^4}{3\mu_0\mu_1\mu_2} \mathbf{F}_{1/2} &= ((\hat{\mu}_1 \cdot \hat{\mu}_2) \hat{d} + (\hat{\mu}_1 \cdot \hat{d}) \hat{\mu}_2 + (\hat{\mu}_2 \cdot \hat{d}) \hat{\mu}_1 - 5(\hat{\mu}_1 \cdot \hat{d})(\hat{\mu}_2 \cdot \hat{d}) \hat{d}) \\ &= (ae+bf+gc) \begin{bmatrix} x \\ y \\ z \end{bmatrix} + (ex+fy+gz) \begin{bmatrix} a \\ b \\ c \end{bmatrix} + (ax+by+cz) \begin{bmatrix} e \\ f \\ g \end{bmatrix} \\ &\quad - 5(ax+by+cz)(ex+fy+gz) \begin{bmatrix} x \\ y \\ z \end{bmatrix} \\ &= \begin{bmatrix} ax & bx & cx \\ ay & by & cy \\ az & bz & cz \end{bmatrix} \begin{bmatrix} e \\ f \\ g \end{bmatrix} + \begin{bmatrix} ax & ay & az \\ bx & by & bz \\ cx & cy & cz \end{bmatrix} \begin{bmatrix} e \\ f \\ g \end{bmatrix} + (ax+by+cz) \begin{bmatrix} e \\ f \\ g \end{bmatrix} \\ &\quad - 5(ax+by+cz) \begin{bmatrix} x^2 & xy & xz \\ xy & y^2 & yz \\ xz & yz & z^2 \end{bmatrix} \begin{bmatrix} e \\ f \\ g \end{bmatrix} \quad (15) \end{aligned}$$

This equation can be simplified in:

$$\mathbf{F}_{1/2} = \frac{3\mu_0}{4\pi d^4} \mu_1 \Phi_1 \mu_2 \quad (16)$$

And it is simple to demonstrate that one can also write:

$$\mathbf{F}_{1/2} = \frac{3\mu_0}{4\pi d^4} \mu_2 \Phi_2 \mu_1 \quad (17)$$

Where Φ_1 is a function of \hat{d} and $\hat{\mu}_1$ defined in equation (11). After some work, one can obtain $\det(\Phi_1(\hat{d}, \hat{\mu}_1)) = -(\hat{\mu}_1 \cdot \hat{d})((\hat{\mu}_1 \cdot \hat{d})^2 + 1)$. Φ_1 can therefore be inverted as long as $(\mu_1 \cdot \hat{d}) \neq 0$. This result will be used later.

β is a function of \hat{d} . As we have $\det(\beta) = 2$, β can therefore be inverted as long as $d > 0$. Its inverse is:

$$\beta^{-1}(\hat{d}) = \frac{1}{2} \begin{bmatrix} 3x^2 - 2 & 3xy & 3xz \\ 3xy & 3y^2 - 2 & 3yz \\ 3xz & 3yz & 3z^2 - 2 \end{bmatrix} \quad (18)$$

6 Electromagnetic navigation

Electromagnetic navigation is a way to determine the relative position and attitude of a target, measuring only the field $\mathbf{B}_{T/C}$ the target dipole creates at the chaser position, and the force $\mathbf{F}_{T/C}$ it induces on the chaser dipole.

Note: The force cannot be measured directly. However, knowing the mass of the chaser, measuring its acceleration enables to get the force $\mathbf{F}_{T/C}$.

6.1 Concept

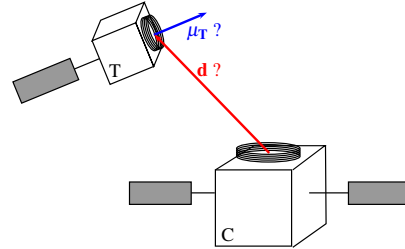


Fig. 2 Navigation problematic. Measuring only its acceleration and the magnetic field surrounding, the chaser can know where the target dipole is.

From equation (14) and (18) we obtain:

$$\mu_T = \frac{4\pi d^3}{\mu_0} \beta^{-1} \mathbf{B}_{T/C} \quad (19)$$

$\mathbf{F}_{T/C} = -\mathbf{F}_{C/T}$ yields:

$$\mathbf{F}_{T/C} = -\frac{3\mu_0}{4\pi d^4} \mu_C \Phi_C \mu_T \quad (20)$$

Combining (19) and (20) finally yields:

$$\mu_C \Phi_C \beta^{-1} \mathbf{B}_{T/C} + \frac{d}{3} \mathbf{F}_{T/C} = 0 \quad (21)$$

Equation (21) can then be completed with equation (9) to form a polynomial system of four equations with four variables (d, x, y, z) . Polynomial systems are a well spread problem, important in many sciences. For this reason, methods have been developed to solve them numerically [11], although no analytical expression of the roots can generally be found.

The best way to proceed is then to use one of the existing methods to find all the roots of the polynomial system. But because our system corresponds to an existing situation, we know that there is at least one root. Therefore, the method used for the moment to find a solution is a simple gradient-based search for the root, using the norm of the left term of equation (21) as cost function.

Once \mathbf{d} found, μ_T is easily obtained from equation (19).

6.2 Results and perspectives

The previous section has developed the method to solve the static navigation problem thanks to magnetic and acceleration measures. It is hence possible to obtain the position of the magnetic dipole, as well as its strength and orientation. Only one degree of freedom is not determined: the rotation around the dipole axis.

This solution is instantaneous: it does not require the configuration to be changing. However, the main difficulty faced would be the calibration of the instruments and the knowledge of the Earth magnetic field. These are varying at a low frequency whereas the measures would vary more quickly, for example because of the tumbling motion of the target. This could be used advantageously with a Kalman filter for instance.

Moreover, using a Kalman filter based on the tumbling motion of the satellite would certainly make it possible to obtain the last degree of freedom, not determined by equation (21).

In order to get rid of the need to know the Earth magnetic field, an other possibility could be to measure the torque created on the chaser and combine several measures. This way, there would be no need for any magnetic field measurement. One could also modify the equations found, in order to measure directly the magnetic field gradient. Then no inertial measurement unit (IMU) would be needed. Both directions should be investigated in the future.

7 Balanced configurations during orbit transfer

The aim of this section is to find a way for the chaser to change the orbit of the formation, while always staying in a balanced geometrical configuration.

7.1 Concept

We will first look for the magnetic force to apply to the chaser and target, in order for the formation to be balanced, even if external forces like propulsion are taken into account, but without trying to ensure a equilibrium attitude for the target. Ensuring this equilibrium attitude will then provide a second equation, enabling to completely solve the problem.

7.1.1 Electromagnetic force for balanced formation

Let's work in an inertial frame. In this frame, we will write:

\mathbf{F}_i	force on i ,
m_i	mass of i ,
\mathbf{f}_i	acceleration: $f_i = \frac{F_i}{m_i}$,
$\boldsymbol{\tau}_i$	torque on i ,
\mathbf{r}_i	vector from the center of the Earth to i center of mass,
\mathbf{s}_i	vector from the system center of mass to i center of mass,
\mathbf{s}	vector from the chaser center of mass to the target center of mass,
\mathbf{d}	vector from the chaser dipole to the target dipole.

We will subscript:

C	chaser satellite,
T	target satellite,
CoM	center of mass of the system target-chaser,
g	gravitation,
$\varepsilon\mu$	electromagnetic,
t	thrusters,
rw	reaction wheels,
p	perturbation.

For example, $\mathbf{F}_{T\varepsilon\mu}$ is the electromagnetic force created by the chaser on the target. Then, the sum of the different forces on i is:

$$\mathbf{F}_i = \mathbf{F}_{ig} + \mathbf{F}_{i\varepsilon\mu} + \mathbf{F}_{it} + \mathbf{F}_{ip} \quad (22)$$

And the sum of the different torques on i is:

$$\boldsymbol{\tau}_i = \boldsymbol{\tau}_{i\varepsilon\mu} + \boldsymbol{\tau}_{it} + \boldsymbol{\tau}_{irw} + \boldsymbol{\tau}_{ip} \quad (23)$$

We have:

$$\mathbf{r}_i = \mathbf{r}_{CoM} + \mathbf{s}_i \quad (24)$$

Let's write the fact that the formation must be balanced:

$$\begin{aligned}
\ddot{\mathbf{s}} &= \ddot{\mathbf{s}}_T - \ddot{\mathbf{s}}_C \\
&= \ddot{\mathbf{r}}_T - \ddot{\mathbf{r}}_C \\
&= \mathbf{f}_{T_g} - \mathbf{f}_{C_g} - \frac{\mathbf{F}_{C_t}}{m_C} + \frac{\mathbf{F}_{T_{\varepsilon\mu}}}{m_T} - \frac{\mathbf{F}_{C_{\varepsilon\mu}}}{m_C} + \Delta\mathbf{f}_p \\
&= \mathbf{f}_{T_g} - \mathbf{f}_{C_g} - \frac{\mathbf{F}_{C_t}}{m_C} + \frac{1}{m_C m_T} (m_C \mathbf{F}_{T_{\varepsilon\mu}} - m_T \mathbf{F}_{C_{\varepsilon\mu}}) + \Delta\mathbf{f}_p \tag{25}
\end{aligned}$$

With $\Delta\mathbf{f}_p = \mathbf{f}_{T_p} - \mathbf{f}_{C_p}$ the difference between the perturbation accelerations felt by the target and the chaser. Knowing that $\mathbf{F}_{T_{\varepsilon\mu}} = -\mathbf{F}_{C_{\varepsilon\mu}}$, equation (25) then yields:

$$\ddot{\mathbf{s}} = \mathbf{f}_{T_g} - \mathbf{f}_{C_g} - \frac{\mathbf{F}_{C_t}}{m_C} + \frac{\mathbf{F}_{T_{\varepsilon\mu}}}{m_{CT}} + \Delta\mathbf{f}_p \tag{26}$$

With:

$$m_{CT} = \frac{m_C m_T}{m_C + m_T} \tag{27}$$

Let's now proceed to a first order approximation of \mathbf{f}_{i_g} , knowing that $s_i \ll r_{CoM}$:

$$\begin{aligned}
\mathbf{f}_{i_g} &= \mathbf{f}_g(\mathbf{r}_i) \\
&= \mathbf{f}_g(\mathbf{r}_{CoM}) + \left. \frac{\partial \mathbf{f}_g}{\partial \mathbf{r}} \right|_{\mathbf{r}=\mathbf{r}_{CoM}} (\mathbf{r}_i - \mathbf{r}_{CoM}) \tag{28}
\end{aligned}$$

Which immediately gives:

$$\begin{aligned}
\mathbf{f}_{T_g} - \mathbf{f}_{C_g} &= \left. \frac{\partial \mathbf{f}_g}{\partial \mathbf{r}} \right|_{\mathbf{r}=\mathbf{r}_{CoM}} (\mathbf{r}_T - \mathbf{r}_C) \\
&= \left. \frac{\partial \mathbf{f}_g}{\partial \mathbf{r}} \right|_{\mathbf{r}=\mathbf{r}_{CoM}} \mathbf{s} \\
&= -\frac{\mu}{r_{CoM}^3} M \mathbf{s} \tag{29}
\end{aligned}$$

With μ the standard gravitational parameter of the Earth. Let's now note $\mathbf{r}_{CoM} = [r_x \ r_y \ r_z]^T$ in the inertial frame. The Jacobian matrix M at \mathbf{r}_{CoM} is obtained from [2]:

$$M = \begin{bmatrix} 1 - 3\frac{r_x^2}{r_{CoM}^2} & 3\frac{r_x r_y}{r_{CoM}^2} & 3\frac{r_x r_z}{r_{CoM}^2} \\ 3\frac{r_x r_y}{r_{CoM}^2} & 1 - 3\frac{r_y^2}{r_{CoM}^2} & 3\frac{r_y r_z}{r_{CoM}^2} \\ 3\frac{r_x r_z}{r_{CoM}^2} & 3\frac{r_y r_z}{r_{CoM}^2} & 1 - 3\frac{r_z^2}{r_{CoM}^2} \end{bmatrix} \tag{30}$$

Finally:

$$\ddot{\mathbf{s}} = -\frac{\mu}{r_{CoM}^3} M \mathbf{s} - \frac{\mathbf{F}_{C_t}}{m_C} + \frac{\mathbf{F}_{T_{\varepsilon\mu}}}{m_{CT}} + \Delta\mathbf{f}_p \tag{31}$$

We will now derive (31) in the orbital frame. Differentiating twice in this frame gives equation (32). In this equation, the rotating frame is starred, to visualise the

difference.

$$\frac{d^2\mathbf{s}}{dt^2} = \frac{d^{*2}\mathbf{s}}{dt^2} + \boldsymbol{\omega} \times (\boldsymbol{\omega} \times \mathbf{s}) + 2\boldsymbol{\omega} \times \frac{d^*\mathbf{s}}{dt} + \frac{d\boldsymbol{\omega}}{dt} \times \mathbf{s} \quad (32)$$

The complete and general equation of the relative motion in the orbital frame is therefore:

$$\frac{d^{*2}\mathbf{s}}{dt^2} + \boldsymbol{\omega} \times (\boldsymbol{\omega} \times \mathbf{s}) + 2\boldsymbol{\omega} \times \frac{d^*\mathbf{s}}{dt} + \frac{d\boldsymbol{\omega}}{dt} \times \mathbf{s} + \frac{\mu}{r_{CoM}^3} M\mathbf{s} = -\frac{\mathbf{F}_{C_t}}{m_C} + \frac{\mathbf{F}_{T_{\epsilon\mu}}}{m_{CT}} + \Delta\mathbf{f}_p \quad (33)$$

In the following, we will assume that the orbit of the center of mass of the formation is circular around the Earth. Equation (33) then becomes:

$$\frac{d^{*2}\mathbf{s}}{dt^2} + \boldsymbol{\omega} \times (\boldsymbol{\omega} \times \mathbf{s}) + 2\boldsymbol{\omega} \times \frac{d^*\mathbf{s}}{dt} + \frac{\mu}{r_{CoM}^3} M\mathbf{s} = -\frac{\mathbf{F}_{C_t}}{m_C} + \frac{\mathbf{F}_{T_{\epsilon\mu}}}{m_{CT}} + \Delta\mathbf{f}_p \quad (34)$$

Let's now look for the equilibrium of the formation. It means that, without restricting the forces applied to each satellite, we will look for equilibrium conditions $\frac{d^{*2}\mathbf{s}}{dt^2} = \frac{d^*\mathbf{s}}{dt} = 0$. The orbital frame being linked directly to \mathbf{r}_{CoM} , $\mathbf{r}_{CoM} = [0 \ 0 \ -r_{CoM}]^T$, and $\boldsymbol{\omega} = [0 \ -n \ 0]^T$. Equation (34) then yields:

$$\boldsymbol{\omega} \times (\boldsymbol{\omega} \times \mathbf{s}) + \frac{\mu}{r_{CoM}^3} M\mathbf{s} = -\frac{\mathbf{F}_{C_t}}{m_C} + \frac{\mathbf{F}_{T_{\epsilon\mu}}}{m_{CT}} + \Delta\mathbf{f}_p \quad (35)$$

Which corresponds to the system:

$$\begin{aligned} 0 &= \frac{F_{T_{\epsilon\mu_x}}}{m_{CT}} - \frac{F_{C_{t_x}}}{m_C} + \Delta f_{p_x} \\ n^2 s_y &= \frac{F_{T_{\epsilon\mu_y}}}{m_{CT}} - \frac{F_{C_{t_y}}}{m_C} + \Delta f_{p_y} \\ -3n^2 s_z &= \frac{F_{T_{\epsilon\mu_z}}}{m_{CT}} - \frac{F_{C_{t_z}}}{m_C} + \Delta f_{p_z} \end{aligned} \quad (36)$$

In the following, we will suppose to simplify that each satellite has its magnetic dipole located at its center of mass. This way, we can write:

$$\mathbf{d} = d\hat{\mathbf{d}} = d [x \ y \ z]^T = \mathbf{s} \quad (37)$$

With \mathbf{d} the vector from the chaser dipole to the target dipole, as defined in section 5.1.

System (37) directly gives the expression of the magnetic force the chaser has to apply on the target in order to stay in a fixed formation:

$$\mathbf{F}_{T_{\epsilon\mu}} = m_{CT} \begin{bmatrix} \frac{F_{C_{t_x}}}{m_C} - \Delta f_{p_x} \\ dn^2 y + \frac{F_{C_{t_y}}}{m_C} - \Delta f_{p_y} \\ -3dn^2 z + \frac{F_{C_{t_z}}}{m_C} - \Delta f_{p_z} \end{bmatrix} \quad (38)$$

In many cases, the orbit transfer rely on a thrust along the V bar axis. If we moreover neglect the perturbation forces, equation (38) becomes for this kind of situations:

$$\mathbf{F}_{T_{\varepsilon\mu}} = m_{CT} \begin{bmatrix} \frac{F_{C_{1x}}}{m_C} \\ dn^2_y \\ -3dn^2_z \end{bmatrix} \quad (39)$$

7.1.2 Balanced attitude during orbit transfer

In order for the transfer to be completely balanced, another criterion is added to equation (35): the attitude of the target in the orbital frame must be in equilibrium also. Let's note B the body frame of the target, I an inertial frame, and O the orbital frame. This gives the constraint:

$$\omega_{B/O} = \mathbf{0} \quad (40)$$

As:

$$\omega_{B/I} = \omega_{B/O} + \omega \quad (41)$$

then:

$$\omega_{B/I} = \omega \quad (42)$$

Writing the rotation of the orbital frame in the satellite natural frame gives:

$$\begin{bmatrix} \omega_1 \\ \omega_2 \\ \omega_3 \end{bmatrix} = P_{O \rightarrow B} \begin{bmatrix} 0 \\ -n \\ 0 \end{bmatrix} \quad (43)$$

With $P_{O \rightarrow B}$ the transition matrix from the orbital frame to the satellite natural frame. Assuming that the attitude of the satellite is described by the three rotations around body axes $C_1(\theta_1) \leftarrow C_2(\theta_2) \leftarrow C_3(\theta_3)$ to B from O , the transition matrix $P_{O \rightarrow B}$ is then given by:

$$P_{O \rightarrow B} = \begin{bmatrix} c\theta_2 c\theta_3 & c\theta_2 s\theta_3 & -s\theta_2 \\ s\theta_1 s\theta_2 c\theta_3 - c\theta_1 s\theta_3 & s\theta_1 s\theta_2 s\theta_3 + c\theta_1 c\theta_3 & s\theta_1 c\theta_2 \\ c\theta_1 s\theta_2 c\theta_3 + s\theta_1 s\theta_3 & c\theta_1 s\theta_2 s\theta_3 - s\theta_1 c\theta_3 & c\theta_1 c\theta_2 \end{bmatrix} \quad (44)$$

where $c\theta_i = \cos(\theta_i)$ and $s\theta_i = \sin(\theta_i)$. Then:

$$\begin{bmatrix} \omega_1 \\ \omega_2 \\ \omega_3 \end{bmatrix} = -n \begin{bmatrix} c\theta_2 s\theta_3 \\ s\theta_1 s\theta_2 s\theta_3 + c\theta_1 c\theta_3 \\ c\theta_1 s\theta_2 s\theta_3 - s\theta_1 c\theta_3 \end{bmatrix} = -n \begin{bmatrix} a \\ b \\ c \end{bmatrix} \quad (45)$$

The evolution of the kinematic momentum of the satellite is then given by:

$$\begin{aligned}
\frac{d}{dt}(J\omega_{\mathbf{B}/\mathbf{I}}) &= J\frac{d\omega_{\mathbf{B}/\mathbf{I}}}{dt} + \omega_{\mathbf{B}/\mathbf{I}} \times J\omega_{\mathbf{B}/\mathbf{I}} \\
&= J\frac{d\omega}{dt} + \omega \times J\omega \\
&= \omega \times J\omega \\
&= -n \begin{bmatrix} a \\ b \\ c \end{bmatrix} \times J \left(-n \begin{bmatrix} a \\ b \\ c \end{bmatrix} \right)
\end{aligned} \tag{46}$$

$$\frac{d}{dt}(J\omega_{\mathbf{B}/\mathbf{N}}) = -\tau_\omega \tag{47}$$

With, in the target natural body frame:

$$\tau_\omega = -n^2 \begin{bmatrix} 0 & -c & b \\ c & 0 & -a \\ -b & a & 0 \end{bmatrix} J \begin{bmatrix} a \\ b \\ c \end{bmatrix} \tag{48}$$

And:

$$\begin{aligned}
\frac{d}{dt}(J\omega_{\mathbf{B}/\mathbf{I}}) &= \sum \tau_{\mathbf{T}} \\
&= \tau_{\mathbf{T}_{\varepsilon\mu}} + \tau_{\mathbf{T}_{\mathbf{p}}}
\end{aligned} \tag{49}$$

Combining equations (49) and (47) finally yields:

$$\tau_{\mathbf{T}_{\varepsilon\mu}} + \tau_{\mathbf{T}_{\mathbf{p}}} + \tau_\omega = \mathbf{0} \tag{50}$$

There are then two ways to solve this equation, which will be developed hereafter.

First method: It is the most straight forward. Indeed, let's suppose $(\hat{\mu}_T \cdot \hat{d}) \neq 0$. We can then invert equation (17):

$$\mu_C = \frac{4\pi d^4}{3\mu_0\mu_T} \Phi_T^{-1} \mathbf{F}_{C/T} \tag{51}$$

Combining equations (49) and (51) with equations (12) and (39) gives:

$$\frac{m_{CT}}{3} d\hat{\mu}_T \times \left(\beta \Phi_T^{-1} \begin{bmatrix} \frac{F_{Cx}}{m_C} \\ d\omega^2 y \\ -3d\omega^2 z \end{bmatrix} \right) + \tau_{\mathbf{p}} + \tau_\omega = \mathbf{0} \tag{52}$$

This equation is a polynomial system. To solve it is not an easy task. Indeed, it can have a infinite number of solution in certain cases. To visualize this, figure 3 represents the norm of the cost function associated to equation (52) for every point in the orbital plane (Oxz). Solutions to equation (52) are located at the places where the cost function is equal to zero. On figure 3, one can easily see that there is a

infinite number of solution to the problem. This indicates that there is a degree of freedom unbound by system (52).

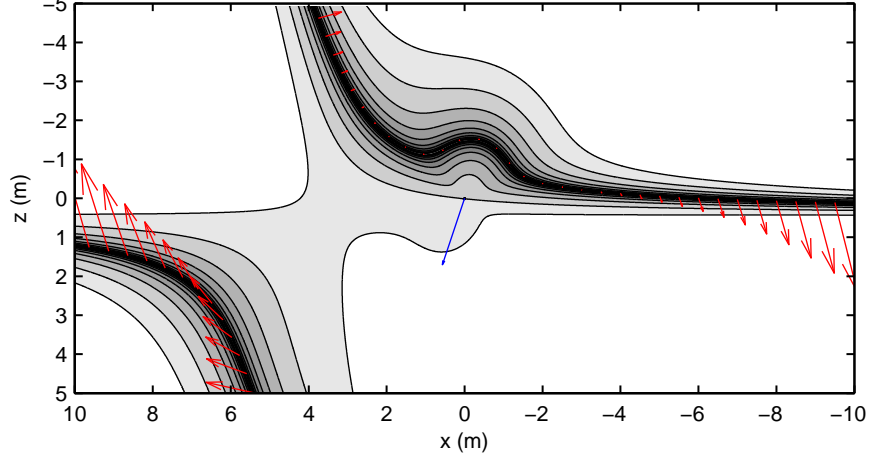


Fig. 3 Representation of possible equilibrium positions. The target is located at the origin of the frame, its magnetic dipole is represented in blue $\mu_T = [94 \ 0 \ 285]^T \text{ Am}^2$. The red vectors represent the chaser dipole associated with some of the possible positions. The frame is the widely used LVLH frame: x is the \mathbf{V} bar vector (collinear to the projection of the velocity vector on a horizontal plane), z is the vertical, toward the Earth, y is perpendicular to the orbital plane. To simplify the problem for this representation, the principal moments of inertia of the target are supposed to be equal. $F_{Clx} = 10 \text{ mN}$ and $\tau_p = [0 \ 3 \ 0]^T \text{ mNm}$. The different masses are : $m_C = 1000 \text{ kg}$, $m_T = 2500 \text{ kg}$. Orbit is circular with $\omega = 1.078 \cdot 10^{-3} \text{ s}^{-1}$.

Second method: the aim is to rewrite the equations in order to take the degree of freedom visible on figure 3 out of the polynomial system. We have:

$$\tau_{T_{\varepsilon\mu}} = \mu_T \times \mathbf{B}_{C/T} \quad (53)$$

Let's decompose $\mathbf{B}_{C/T}$ in $\mathbf{B}_{C/T_{\perp}} + \mathbf{B}_{C/T_{\parallel}}$, with $\mathbf{B}_{C/T_{\perp}} \perp \mu_T$ and $\mathbf{B}_{C/T_{\parallel}} \parallel \mu_T$. Then (53) is equivalent to:

$$\tau_{T_{\varepsilon\mu}} = \mu_T \times \mathbf{B}_{C/T_{\perp}} \quad (54)$$

We can then write:

$$\begin{aligned} \|\tau_{T_{\varepsilon\mu}}\| \hat{\tau}_{T_{\varepsilon\mu}} &= \|\mu_T\| \|\mathbf{B}_{C/T_{\perp}}\| \hat{\mu}_T \times \hat{B}_{C/T_{\perp}} \\ \hat{\tau}_{T_{\varepsilon\mu}} &= \hat{\mu}_T \times \hat{B}_{C/T_{\perp}} \\ \hat{B}_{C/T_{\perp}} &= \hat{\tau}_{T_{\varepsilon\mu}} \times \hat{\mu}_T \\ \|\mu_T\| \|\mathbf{B}_{C/T_{\perp}}\| \hat{B}_{C/T_{\perp}} &= \|\tau_{T_{\varepsilon\mu}}\| \hat{\tau}_{T_{\varepsilon\mu}} \times \hat{\mu}_T \\ \mathbf{B}_{C/T_{\perp}} &= \tau_{T_{\varepsilon\mu}} \times \frac{\mu_T}{\mu_T^2} \end{aligned} \quad (55)$$

To satisfy equation (49), one can then chose $k \in \mathbb{R}$ in order to have:

$$\mathbf{B}_{C/T} = \boldsymbol{\tau}_{T_{\varepsilon\mu}} \times \frac{\boldsymbol{\mu}_T}{\mu_T^2} + k \frac{\boldsymbol{\mu}_T}{\mu_T^2} \quad (56)$$

k is then homogeneous to a torque. Equation (49) yields:

$$\mathbf{B}_{C/T} = (-\boldsymbol{\tau}_{T_p} - \boldsymbol{\tau}_\omega) \times \frac{\boldsymbol{\mu}_T}{\mu_T^2} + k \frac{\boldsymbol{\mu}_T}{\mu_T^2} \quad (57)$$

We can then finally obtain the dipole the chaser has to create in order to balance the torques on the target thanks to equation (14):

$$\boldsymbol{\mu}_C = \frac{4\pi d^3}{\mu_0} \beta^{-1} \left(\frac{\boldsymbol{\mu}_T}{\mu_T^2} \times (\boldsymbol{\tau}_{T_p} + \boldsymbol{\tau}_\omega) + k \frac{\boldsymbol{\mu}_T}{\mu_T^2} \right), \text{ with } k \in \mathbb{R} \quad (58)$$

As we have:

$$\mathbf{F}_{T_{\varepsilon\mu}} = \frac{3\mu_0}{4\pi d^4} \mu_T \Phi_T \boldsymbol{\mu}_C \quad (59)$$

We can directly derive:

$$\mu_T \Phi_T \beta^{-1} \left(\frac{\boldsymbol{\mu}_T}{\mu_T^2} \times (\boldsymbol{\tau}_{T_p} + \boldsymbol{\tau}_\omega) + k \frac{\boldsymbol{\mu}_T}{\mu_T^2} \right) - \frac{m_C r d}{3} \begin{bmatrix} \frac{F_{C_x}}{m_C} \\ d\omega^2 y \\ -3d\omega^2 z \end{bmatrix} = 0, \text{ with } k \in \mathbb{R} \quad (60)$$

We can then finally simplify this equation to obtain:

$$\Phi_T \beta^{-1} (\hat{\boldsymbol{\mu}}_T \times (\boldsymbol{\tau}_{T_p} + \boldsymbol{\tau}_\omega) + k \hat{\boldsymbol{\mu}}_T) - \frac{m_C r d}{3} \begin{bmatrix} \frac{F_{C_x}}{m_C} \\ d\omega^2 y \\ -3d\omega^2 z \end{bmatrix} = 0, \text{ with } k \in \mathbb{R} \quad (61)$$

Equation (61), completed with equation (9), is again a polynomial system of four variables (d, x, y, z) composed of four equations. Solving it provides all the possibilities for a balanced formation orbit transfer. The degree of freedom previously causing the number of solutions to be infinite is this time represented by variable k .

Note: Both methods enable to compensate the perturbation torque on the target, if this torque has no component along the target dipole axis. However, there is no constraint on the magnetic torque applied by the target on the chaser.

To sum up, the previous section has developed the equations needed to find the possible configurations enabling to change the absolute orbit of a semi-cooperative EMFF. Indeed, equation (61) is a polynomial system, which roots represent the positions the chaser has to adopt relatively to the target, in order to create an absolute acceleration while keeping the formation in equilibrium.

7.2 Results and perspectives

Figure 4 presents the results found when solving system (61) with a continuation method: k varies continuously, and for each value of k an optimisation is realised. In this figure, only the solutions in the orbital plane were kept, in order to easily represent them. Out-of-plane solutions exist. It is interesting to note that system (61)

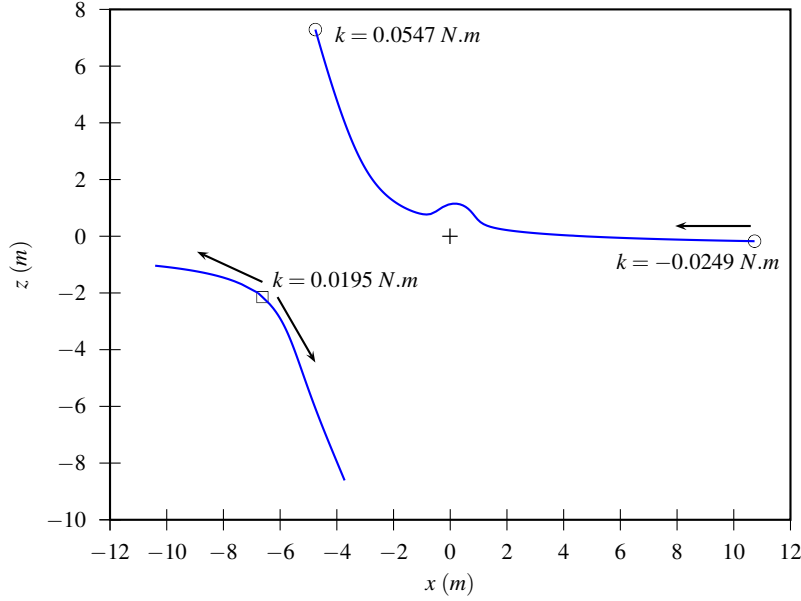


Fig. 4 Solutions of equation (61), found using a continuation method. The parameters are the same as the one used in figure 3. The cross is the position of the target: at the center of the frame. The arrows indicate the direction in which k increases. The square is the place where the second root appears, and then divides into two. It corresponds to the point $k \simeq 0.0195 Nm$ in figure 5 where the number of solutions for μ_C passes from one to three. The limits of the solutions are chosen in order to constrain $\|\mu_C\| \leq 10^6 Am^2$, as is can be seen in figure 5

does not depend from $\|\mu_T\|$. Therefore, the geometrical configuration of the formation during an orbit transfer depends essentially on the orientation of the target dipole. However, the norm of the target dipole has an impact on the norm of the chaser dipole: both are inversely proportional. Therefore, a target dipole too weak implies a very strong chaser dipole. If the dipole needed overcomes the chaser capacity, the distance d between the two coils must be reduced. This on the other hand impacts the formation geometrical configuration.

Figure 5 presents the norm of the chaser dipole, associated with the solutions found in figure 4. For some values of k , several solutions exist to equation (61).

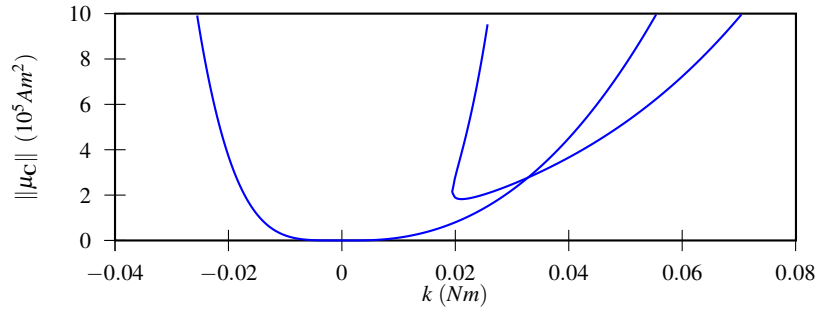


Fig. 5 Norm of the chaser dipole associated with the solutions found in figure (4). One can see on this graph that the number of possible configurations depends on the maximal dipole which can be created by the chaser. If this limit is below $2 \cdot 10^5 \text{ Am}^2$, only two configurations exist for each value of $\|\mu_C\|$. If on the contrary $\|\mu_C\| > 2 \cdot 10^5 \text{ Am}^2$, four different configurations exist.

Having the possibility to choose the value of k provides a way to optimise the formation configuration during the orbit transfer. Several parameters would be interesting to optimize. For example, the value and direction of the chaser dipole would directly impact the perturbation torques applying on this satellite, due to the Earth magnetic field. This perturbation torque, or its mean value during an orbit, would be a good optimization candidate.

8 Conclusions and future work

This study aims to perform magnetic GNC for formation flying satellites. Toward this end, sections 6 and 7 have developed the equations used to solve the navigation and guidance during a formation orbit transfer. These equations are very similar, thanks to the model used to describe the magnetic interactions between the two satellites at stake. Both are polynomial systems, which solutions can be found either using special methods, or with gradient descent optimisations of the cost function associated.

Section 6 has showed that it is possible to have an estimation of the target attitude, using only the acceleration of the chaser, and the magnetic field created by the target. These measures are interesting when compared to standard non-cooperative navigation measurement. Indeed, while cameras can be affected by luminosity, acceleration and magnetic field cannot. Much work remains to be done on the subject. The impact of the magnetic model imperfections has to be assessed. Moreover, filtering the results would certainly improve this navigation method.

Section 7 has showed that balanced configurations in which the formation's orbit can be modified exist. These configurations ensure the equilibrium of the formation during the transfer. Of course, the stability of these configurations should be assessed. Once this done, control laws must be written and demonstrated in order to

stabilize the formation. This represents the future work concerning formation guidance and control during orbit modification.

References

1. Ahsun, U.: Dynamics and control of electromagnetic satellite formations. Ph.D. thesis, Massachusetts Institute of Technology (2007)
2. Ankersen, F.: Guidance, navigation, control and relative dynamics for spacecraft proximity maneuvers: Ph.D. thesis. Aalborg University (2011)
3. Brown, O., Long, A., Shah, N., Eremenko, P.: System lifecycle cost under uncertainty as a design metric encompassing the value of architectural flexibility. In: AIAA SPACE 2007 Conference and Exposition. American Institute of Aeronautics and Astronautics (2007)
4. Buck, A.J.: Path planning and position control of an underactuated [sic] electromagnetic formation flight satellite system in the near field (2013)
5. Camillo, P.J., Markley, F.L.: Orbit-averaged behavior of magnetic control laws for momentum unloading. *Journal of Guidance, Control, and Dynamics* **3**, 563–568 (1980)
6. Dargent, T., Maini, M.: Magnetic actuator in space and application for high precision formation flying. Tech. rep. (2005)
7. Delpéch, M., Berges, J.C., Karlsson, T., Malbet, F.: Results of PRISMA/FFIORD extended mission and applicability to future formation flying and active debris removal missions. *International Journal of Space Science and Engineering* **1**, 382–409 (2013)
8. Kong, E.M., Kwon, D.W., Schweighart, S.A., Elias, L.M., Sedwick, R.J., Miller, D.W.: Electromagnetic formation flight for multisatellite arrays. *Journal of Spacecraft and Rockets* **41**, 659–666 (2004)
9. Kwon, D.W.: Electromagnetic formation flight of satellite arrays. Ph.D. thesis, Massachusetts Institute of Technology (2005)
10. Miller, D.W., Sedwick, R.J., Kong, E.M., Schweighart, S.: Electromagnetic formation flight for sparse aperture telescopes. In: Aerospace Conference Proceedings, pp. 2–729. IEEE (2002)
11. Morgan, A.: Solving Polynomial Systems Using Continuation for Engineering and Scientific Problems. SIAM (2009)
12. Reynerson, C.: Spacecraft modular architecture design for on-orbit servicing. In: 2000 IEEE Aerospace Conference Proceedings, vol. 4, pp. 227–238 vol.4 (2000)
13. Sakai, S.i., Kaneda, R., Maeda, K., Saitoh, T., Saito, H., Hashimoto, T.: Electromagnetic formation flight for LEO satellites. In: Proceedings of the 17th Workshop on JAXA Astrodynamics and Flight Mechanics (2008)
14. Schweighart, S.A.: Electromagnetic formation flight dipole solution planning. Ph.D. thesis, Massachusetts Institute of Technology (2005)
15. Stickler, A.C., Alfriend, K.: Elementary magnetic attitude control system. *Journal of Spacecraft and Rockets* **13**, 282–287 (1976)
16. Torisaka, A., Ozawa, S., Yamakawa, H., Kobayashi, N.: Position and attitude control of formation flying satellites for restructuring their configurations by electromagnetic force at the docking phase. American Institute of Aeronautics and Astronautics (2013)
17. Villani, D.D.: An analytic solution for the force between two magnetic dipoles. *Magnetic and Electrical Separation* **9**, 39–52 (1998)
18. Voirin, T., Kowaltschek, S., Dubois-Matra, O.: NOMAD: a contactless technique for active large debris removal. IAC-12 (2012)